Acoustical Properties of Porous Asphalts: Theoretical and Environmental Aspects

M. BERENGIER, J. F. HAMET, AND P. BAR

The acoustical aspects of porous road surfaces as studied in France are described in this paper. The first part discusses the advantages of porous asphalt and shows how and why, in France, two experimental approaches are carried out: thin porous layers (~4 cm) for the interurban and urban network, and thick porous layers (40 to 50 cm) for the urban network. The second part presents a theoretical model: the absorption coefficient as a function of frequency is obtained from the layer thickness and three physical parameters representative of the porous medium. The influence of these parameters on the absorption is described. It is clearly shown that above a certain value, thickness has no influence on the absorption properties (i.e., increasing the thickness becomes acoustically useless). This is called the "superthickness" condition. In the third part, experimental results obtained in the laboratory and in situ are compared with the theoretical calculations. The influences of humidity, gaps in the grading, binder content, and number of layers are also presented. The last part deals with noise reduction as measured with rolling vehicles (pass by, coast by). Experimental programs in progress are described and some results are given. Evolution of noise level versus road aging is also discussed.

In the last 10 years, vehicle noise has been substantially reduced. For light vehicles, the maximum noise level decreased from 81 dB(A) in 1982 to 77 dB(A) in 1988, and for heavy vehicles, from 91 dB(A) to 84 dB(A) (measurements performed following the ISO R 362) (*1*).

These important noise reductions have been primarily obtained by reducing engine noise, developing a better conception of transmission, and constantly improving silencers. In these conditions, the rolling noise tends to predominate, particularly on expressways and uncongested urban roads where the traffic speed exceeds 50 km/hr. This is especially the case at night, when traffic noise is the most disturbing (i.e., in its effects on sleep).

The spread of noise levels measured on different road and vehicle configurations can reach 10 dB(A) (*1–3*). Therefore, it is worthwhile to reduce traffic noise by an appropriate conception of pavements, particularly the wearing course.

In urban areas, where management of vehicle flow is not sufficient to significantly lower noise levels, it is not possible to consider noise protection devices such as barriers: acoustical improvement of building facades has been until now the only way to protect dwellings from traffic noise. It is, however, just a partial solution because it is efficient inside, but only with closed windows. A reduction of several decibels in noise emission itself, because of a suitable pavement, would be real progress (*4*).

In a periurban area, a noise-reducing pavement would make it possible to avoid excessively high noise barriers. This presents two advantages: (a) better integration into the landscape and (b) lower cost [noise barriers cost about 2000 FF (U.S. $300)/m^2 and the amount usually increases with height].

Such road surfaces might also complement efforts by car manufacturers to reduce the noise inside the vehicle.

EXPERIMENTAL APPROACHES

The use of porous asphalts for wearing courses has been explored for about 20 years. The use of new binders and the results of research on the acoustic efficiency of these pavements can explain recent developments.

In France (*5*), two experimental approaches have been carried out. One is a thin porous asphalt wearing course (about 4 cm thick) combined with an integral porous structure from the road subbase to the surface (about 40 to 50 cm thick). The thin porous layer is used on both interurban and urban networks. In the interurban domain, several experiments are in progress to determine adequate formulations and study the problems of aging and maintenance. Numerous experimental tracks have been established in various places in France, for instance,

- In 1986–1987, 200 km on the heavily trafficked A1 Motorway between Paris and Lille, and
- In 1988, 20 km between Orléans and Vierzon, and 18 experimental tracks (500 m long) on A 63 (Bordeaux-Bayonne) where different thicknesses (2.5 cm to 6 cm), binders, and gradings (0/10, 0/14, 0/20) have been tested. On the latter site, gripping, evenness, and texture were measured simultaneously with the acoustic measurements. During the next few years, a follow-up study will be carried out in order to control how these pavements behave over time.

The second approach, a thick porous structure, represents more ambitious research. These structures are built similarly to "reservoir pavements," whose purpose is to absorb rainwater and delay water flow evacuation (i.e., during heavy rains). One site is located near Nantes, France. A second site, experimental, is situated in the Lyon area. In this case, properties of thick structures were theoretically evaluated by using the model discussed later (*6*, *7*) and experimentally confirmed (*8*). Following this work, four experimental tracks (50 m long) were built during the summer of 1989. Three are 40 cm thick and one is 50 cm thick. Several gradings between 0/10 and

M. Berengier, Laboratoire Central des Ponts et Chaussées, BP 19, 44340 Bouguenais, France. J. F. Hamet, Institut National de Recherche sur les Transports et leur Sécurité, 109, Avenue S. Allende, 69675 Bron Cédex, France. P. Bar, Centre d'Etude des Transports Urbains, 8, Avenue A. Briand, 92223 Bagneux, France.

0/20 and binders (pure and modified bitumen and hydraulic, or porous, concrete) were used. A first set of measurements is in progress. A follow-up of the behavior under winter conditions is also planned in order to ensure correct maintenance. The first results will be published in 1990.

ADVANTAGES OF POROUS ASPHALTS

It is now established by specialists on rolling noise and confirmed by recent experiments carried out in several countries that porous asphalts (4 cm thick, 15 to 20 percent voids) provide noise attenuation relative to classical surfaces and dressings (*3*) whose values fluctuate between 3 and 6 dB(A). Their main advantages are to

- Reduce the noise emission (exterior noise), which can be particularly attractive in urban areas;
- Reduce noise inside vehicles;
- Reduce vibrations inside vehicles, which can increase the level of comfort for the users and the electronic devices;
- Reduce water splash and spray (which is a safety factor);
- Improve skid resistance on wet pavement in the high-speed domain, and
- Provide temporary water storage.

These qualities must not mask some problems with winter maintenance that must be adapted to the specificity of such pavements. In other respects, some questions must still be answered about layer optimization, the mechanical behavior of the structure under heavy traffic (resistance to rutting and clogging), and finally water flow in urban road systems.

Because of these qualities, porous asphalt will probably be more extensively used in urban and periurban networks.

MODEL FOR ACOUSTICAL PROPERTIES OF POROUS ROADS

The acoustic absorption coefficient of a road surface representing the proportion of acoustic energy not reflected by this surface for a monochromatic plane wave impinging normally on it is referred to here as absorption coefficient a_0.

First, a brief review of how a_0 can be determined from acoustical characteristics of the media (for a multilayered system) is given. Then how these acoustical characteristics are obtained from physical parameters, how to measure these parameters, and how the physical parameters influence the absorption coefficient are reviewed.

Absorption Coefficient and Acoustical Characteristics

The absorption coefficient a_0 of a surface can be determined from the acoustic impedance Z (complex quantity) of this surface (Equation 1). For a layer of thickness e backed by an impedance Z_T, the surface impedance is given by Equation 2.

$$a_0 = 1 - \frac{|Z - \rho c|^2}{|Z + \rho c|^2} \tag{1}$$

$$Z = W \frac{Z_T \coth\gamma e + W}{Z_T + W \coth\gamma e} \tag{2}$$

where

ρc = characteristic air impedance,
W = characteristic impedance, and
γ = propagation constant.

W and γ are the acoustical characteristics of the medium.

Remark. The complex convention adopted in this paper for harmonic time dependence is $e^{i\omega t}$.

Equation 2 is used to evaluate, through an iterative procedure, the surface impedance of a multilayered system: one needs to know the W and γ for each layer and the end (bottom) impedance of the system.

Acoustical Characteristics and Physical Parameters

The acoustical characteristics W and γ of a porous medium can be obtained from physical parameters. For the case of mineral fibers, Delany and Bazley (*9*) have shown that the only physical parameter to consider was the specific airflow resistance R_S. Various authors have tried to extend these results to other media such as soil (or sand, asphalt, etc.) in the presence of snow or vegetation. Predictions and measurements did not always agree. An explanation is that acoustic characteristics of a medium do not depend only on the airflow resistance (friction forces) but also on the porosity (proportion of air in the medium) and on the path the air has to follow (between the fibers, the particles, etc.) (*10*). The fiber materials studied by Delany and Bazley had a porosity near unity and an air path almost unaffected by the presence of fibers.

For porous roads, the medium is assimilated to a homogeneous fluid. The solid structure is supposed rigid, nonmoving. This approach is a macroscopic one: the dimensions of pores and particles must be small enough with respect to the wavelength (which in air is ~17 cm at 2,000 Hz). This limits the validity of the model up to about a few kilohertz.

The fundamental equations of state, continuity, and motion are used to evaluate, at each frequency, the acoustical characteristics W and γ from three physical parameters representative of the medium. The general philosophy follows Morse and Ingard (*11*). The equation formulations are given elsewhere (*10*). Details have been given by Hamet (*6*). The results are [compare work by Von Meier (*12*)]

$$W = \rho c \frac{\sqrt{K}}{\Omega}\left(1 - i\frac{R_S}{\omega\rho}\frac{\Omega}{K}\right)^{1/2} \tag{3}$$

$$\gamma = i\frac{\omega}{c}\sqrt{K}\left(1 - i\frac{R_S}{\omega\rho}\frac{\Omega}{K}\right)^{1/2} \tag{4}$$

where

Ω = porosity ($\Omega \leq 1$),
R_S = specific airflow resistance, and
K = shape factor ($K \geq 1$).

Porosity Ω

The porosity is introduced in the continuity equation, which states that the rate of mass increase of air in a volume results

from a mass flux of air through the surface limiting the volume. If it is stated that the air occupies a fraction ΩdV of the elementary volume dV, the equation reads

$$\iiint \frac{\partial \rho}{\partial t}\,\Omega dV = -\iint \rho u \cdot dS$$

where ρ is the density of the fluid and $u \cdot dS$ is the volume flow rate of the fluid through the surface dS normal to this surface (taken > 0 for outward flow).

From this formulation, it is clear that the porosity Ω must correspond to connected pores and is therefore defined as

$$\Omega = \frac{\text{volume of connected pores}}{\text{total volume}}$$

The porosity is actually measured with a gamma-ray technique (*13*). It is therefore implicitly assumed that the measured "air volume" corresponds to connected pores, which is reasonable because the porous medium is made of (asphalt) coated particles.

Specific Air Flow Resistance R_S

The equation of motion takes into account the "frictional retardation to flow through the pores" (*14*). In the x-direction, the equation reads

$$R_S\, u = -\frac{\partial p}{\partial x} \tag{5}$$

where p is the acoustic pressure in the medium and u is the volume flow rate in the x-direction.

R_S can be measured using a steady flow technique (*14*):

$$R_S = \frac{1}{u_c}\frac{\Delta P}{e} \tag{6}$$

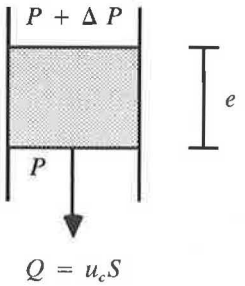

If ΔP is the pressure difference created between the two faces of a layer of thickness e and $u_c = Q/S$ is the steady volume flow rate of fluid per unit area through the sample, one gets R_S from Equation 6.

Remark 1. In order for the measurement conditions for Equation 6 to correspond to the acoustic conditions for Equation 5, the flow velocity u_c must be sufficiently small (laminar flow conditions (*14*). If not, R_S will depend on the velocity u_c, as can be seen from Figure 1.

Remark 2. R_S is expressed in Nm^4 in the mks system. The cgs system with the unit rays per centimeter is used here. (1 rayl/c = $1kN/m^4$.)

Shape Factor K

The shape factor is used to take into account the facts that

- The air paths through the layer do not always follow the normal direction (they are more or less tortuous), and
- The pore cross-sections can vary along the paths.

It is introduced in the inertial term of the equation of motion in the following way:

$$K\rho \frac{\partial u_{\text{pore}}}{\partial t} = -\frac{\partial p}{\partial x} \qquad K \geq 1 \tag{7}$$

where u_{pore} is the average velocity of the air in the pores in the x-direction (average taken over the surface normal to x). It is related to the average flow rate per unit area u by the relation $\Omega\, u_{\text{pore}} = u$.

If one considers both the inertial term (Equation 7) and the friction term (Equation 5), the equation of motion reads

$$\frac{K}{\Omega}\rho \frac{\partial u}{\partial t} + R_S\, u = -\frac{\partial p}{\partial x}$$

The authors do not know of any direct way to measure the shape factor K. It is indirectly determined from the absorption curve measured for a single layer of material, as will be indicated later.

Relations Between Physical Parameters

Each physical parameter has been introduced to take into account given physical phenomena:

- Relative air volume ($0 < \Omega < 1$),
- Flow resistance to motion (R_S), and
- Inertial modifications ($K > 1$).

As will be seen, each parameter has a specific effect on the absorption coefficient. This does not mean that these parameters are otherwise independent of each other.

The following relation, for instance, is proposed for aggregate media (*15*):

$$R_S = A\,\frac{\tau}{\Omega^3\, d^2}$$

where τ is tortuosity and d is the particle diameter.

Tortuosity quantifies the average developed length (l_d) of a flow path between the two faces of a sample, with respect to the actual distance (l_m) between two faces: $r = l_d/l_m \geq 1$.

Acoustic Absorption of Porous Asphalt

General observations can be made for the case of single layers only.

The porous asphalt is laid on an impervious surface whose acoustic impedance is practically infinite. The surface impedance of the layer is obtained from Equation 2 by solving $Z_T = \infty$. One obtains

$$Z = W \coth \gamma e \tag{8}$$

where W and γ are given by Equations 3 and 4.

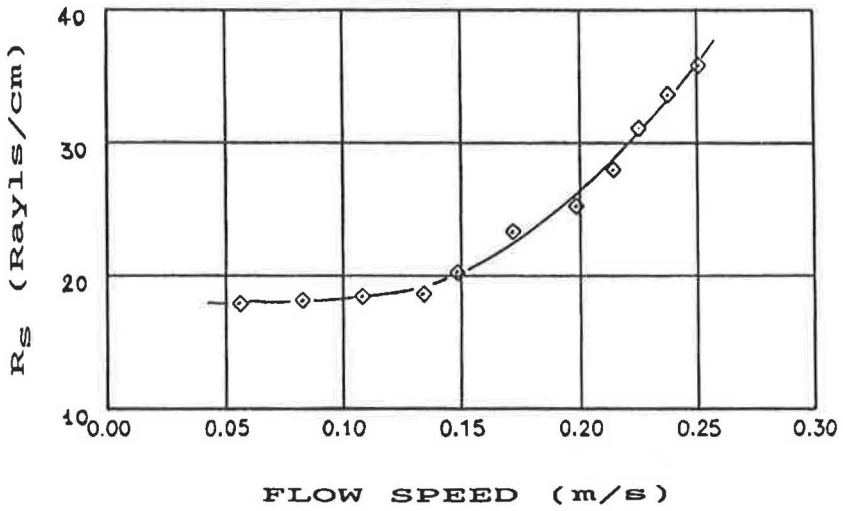

FIGURE 1 Measured R_S (rayls/cm) as function of u_c (m/sec).

If one defines a critical frequency,

$$f_c = \frac{1}{2\pi} \frac{R_S}{\rho} \frac{\Omega}{K}$$

These relations can be written

$$W = \rho c \frac{\sqrt{K}}{\Omega} \left(1 - i\frac{f_c}{f}\right)^{1/2} \tag{9}$$

$$\gamma = i\frac{\omega}{c} \sqrt{K} \left(1 - i\frac{f_c}{f}\right)^{1/2} \tag{10}$$

For example, for porous asphalt with $R_S = 20$ rayls/cm, $\Omega = 0.20$, and $K = 3.5$ (which are usual values), one gets $f_c = 150$ Hz.

In the domain $f >> f_c$ the following approximations can be made:

$$W = R + iX \qquad \frac{R}{\rho c} \approx \frac{\sqrt{K}}{\Omega} \qquad \frac{X}{\rho c} \approx -\frac{1}{2} \frac{1}{\sqrt{K}} \frac{R_S}{\omega \rho} \tag{11}$$

$$\gamma = \alpha + i\beta \qquad \alpha \approx \frac{1}{2} \frac{\Omega}{\sqrt{K}} \frac{R_S}{\rho c} \qquad \beta \approx \frac{\omega}{c} \sqrt{K} \tag{12}$$

These approximations will often be used in the analysis. The absorption curves, however, will always be calculated using the exact formulations (Equations 3 and 4).

Influence of the Total Airflow Resistance $R_T = R_S e$

One can show (*6*) that the absorption coefficient dependence is of the form

$$a_0 \equiv a_0 \left(K, \Omega, \frac{R_T}{\rho c}, \frac{f}{f_c}\right)$$

If R_S and e vary in such a way that $R_T = R_S \cdot e$ = constant, there will be

- No modification of the curves' shape, and
- A simple frequency translation (in logarithmic scale) of the curves.

An illustration is given in Figure 2 for a layer with R_T = 200 rayls.

Remark. A rayl cgs = 10 rayls mks. For example, ρc = 41.5 rayls cgs = 415 rayls mks.

These curves are typical: the absorption coefficient starts from low values at low frequencies, then increases steadily to a maximum value, and oscillates afterwards as frequency increases.

In the $f >> f_c$ domain the maximum value is given by

$$a_{0\ \max} = 1 - \left(\frac{D - 1}{D + 1}\right)^2 \qquad \text{with}$$

$$D = \frac{\sqrt{K}}{\Omega} \tanh \left(\frac{\Omega}{\sqrt{K}} \frac{R_T}{2\rho c}\right) \tag{13}$$

For most of the materials tested, the Ω and K-values observed were such that $\Omega/\sqrt{K} < 0.2$. In consequence, the $a_{0\ \max}$ value reaches unity if $R_T \approx 2\ \rho c = 83$ rayls and $a_{0\ \max} > 0.95$ if $0.7 < R_T/2\rho c < 1.4$, that is, $58 < R_S \cdot e < 116$ rayls cgs. About $a_{0\ \max} = 1$, the maximum value of absorption is not very sensitive to R_T variation.

For very low R_T, *the maximum value of absorption is low. It increases with* R_T *and reaches unity for* $R_T \approx 2\ \rho c = 83$ *rayls cgs. For higher values of* R_T *it diminishes and tends to the asymptotic value*

$$a_{0\ \text{asympt}} = 1 - \left(\frac{\sqrt{K}/\Omega - 1}{\sqrt{K}/\Omega + 1}\right)^2 \tag{14}$$

Single Layers with Low Thickness

The oscillations of the absorption coefficient with frequency come from the coth (γe) term in Equation 8. For a high enough thickness, this term tends to unity and $Z \approx W$. Thus it is

possible to say that the "superthickness" condition has been reached. This case will be treated later. First thicknesses such that coth γe is not close to unity are considered. The absorption curve presents oscillations.

Influence of Specific Airflow Resistance R_S From the earlier analysis, R_S influences the shape of the curve. In the domain $R_S\ e/2\rho c < 1$, an increase of R_S will increase the $a_{0\ max}$ value, which will reach unity when $R_S \approx 2\ \rho c/e$ and then, as R_S increases, will decrease to reach ultimately the asymptotic value (Equation 14). An illustration is given in Figure 3.

The three curves correspond to $R_T = 200$, 400, and 600 rayls, respectively, that is, to $R_T > 2\ \rho c = 83$ rayls. The increase of R_S tends to decrease the $a_{0\ max}$ values and increase the minimum values: the curves have a tendency to "flatten."

Relating to R_S influence, one notes that the frequencies at which the maxima of absorption occur are not modified by R_S. This is typical: later it can be seen that these frequencies depend only on K and e.

Influence of Porosity Ω From Equation 13 (high-frequency approximation) and taking into account that, for most of the materials tested, it was found that $\Omega/\sqrt{K} < 0.2$, one sees that

- For not too high values of $R_T/2\rho c$, the porosity has almost no influence on the maximum values of absorption, and
- The Ω influence on maximum values becomes important for very large $R_T/2\rho c$ (cf. Equation 14).

Large $R_T/2\rho c$ usually means large thicknesses. This case will be considered in the "superthickness" case. For usual cases, the situation is as shown in Figure 4.

The increase of porosity from 0.1 to 0.3 widens the curves in the vicinity of the maximum values, and increases the

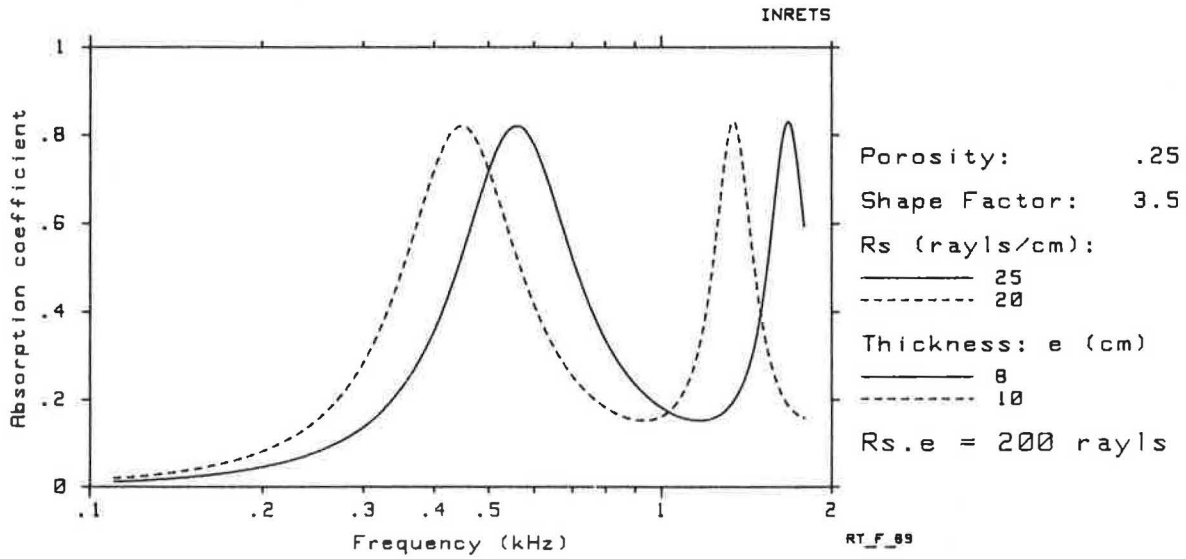

FIGURE 2 Influence of R_S and e on absorption with $R_T = R_S e = 200$ rayls.

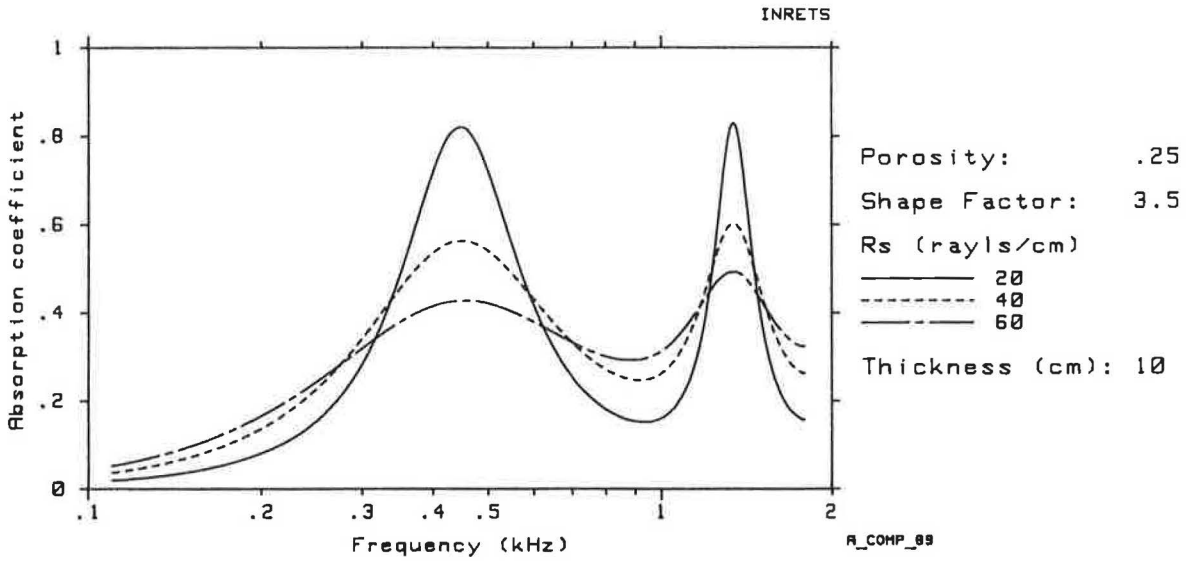

FIGURE 3 Influence of R_S on absorption coefficient.

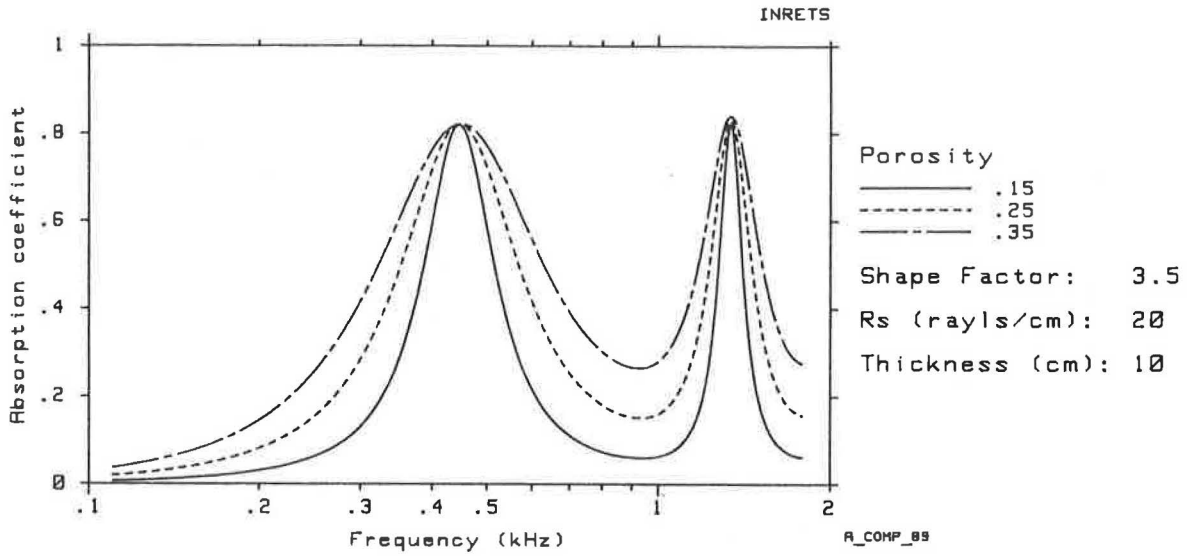

FIGURE 4 Influence of porosity on absorption with $R_T/2\rho c \approx 2.4$, that is, not too large.

minimum values. It has almost no effect on the maximum values and no effect on the frequencies at which these values occur.

A high porosity favors a high absorption between the maximum values.

Influence of the Shape Factor K With the high high-frequency approximations (Equations 11 and 12), one finds (*6*) that the maximum values of absorption occur at frequencies such that

$$f_{2n+1} = (2n + 1)\frac{c/\sqrt{K}}{4e} \qquad n = 0, 1, 2, \ldots \tag{15}$$

frequencies that depend only on the shape factor K and on the thickness e. This result is used to determine K (compare Figure 5).

$$K = \left[\frac{2n + 1}{4}\frac{c}{ef_{n+1}}\right]^2 \qquad n = 0, 1, 2, \ldots \tag{16}$$

Experimental observations show that the estimated K

- Does not depend on the value of n, and
- Does not depend, for a given material, on the thickness of the layer. This implies that the layers are homogeneous (the characteristics are independent of the thickness).

Concerning the influence of K on the absorption curves, it can be said that (see Figure 6)

- A variation in K modifies the frequency positions of the absorption peaks (Equation 19),
- K has almost no influence on the value of the peaks [for not too high values of $R_T/2\ \rho c$ (Equation 13)], and
- An increase in K narrows the width of the curves in the vicinity of the maximums of absorption and decreases the minimum values of absorption (effect opposite to the Ω influence, Equation 13).

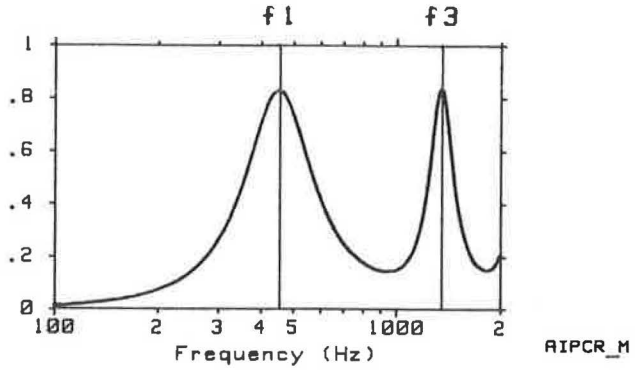

FIGURE 5 Maximum values of absorption occur at frequencies f_1 and f_3.

Influence of Thickness e Thickness has an effect on

- The shape of the absorption curve, and
- The frequencies at which the maxima occur—increasing the thickness lowers these frequencies (Equation 15).

As for the R_S case, an increase of e will increase the a_{0max} values (as long as $R_S e < 2\rho c = 83$ rayls) until unity (when $R_S e = 83$ rayls). As e still increases, a_{0max} will decrease to the asymptotic value (Equation 14). An illustration is given in Figure 7.

Superthickness (7)

When the thickness becomes large enough, coth $(\gamma e) \rightarrow 1$ and $Z \rightarrow W$. The absorption no longer depends on thickness. This is called the superthickness condition. Increasing e further will have no effect on the absorption coefficient given by

$$a_0 = 1 - \left|\frac{W/\rho c - 1}{W/\rho c + 1}\right|^2 \tag{17}$$

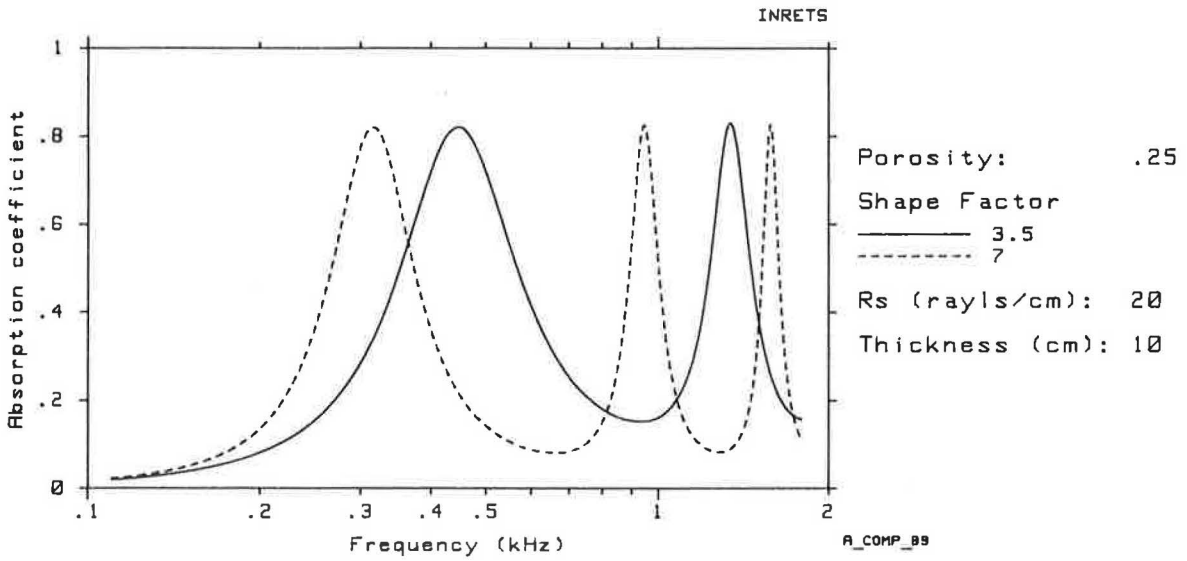

FIGURE 6 Influence of the shape factor on absorption.

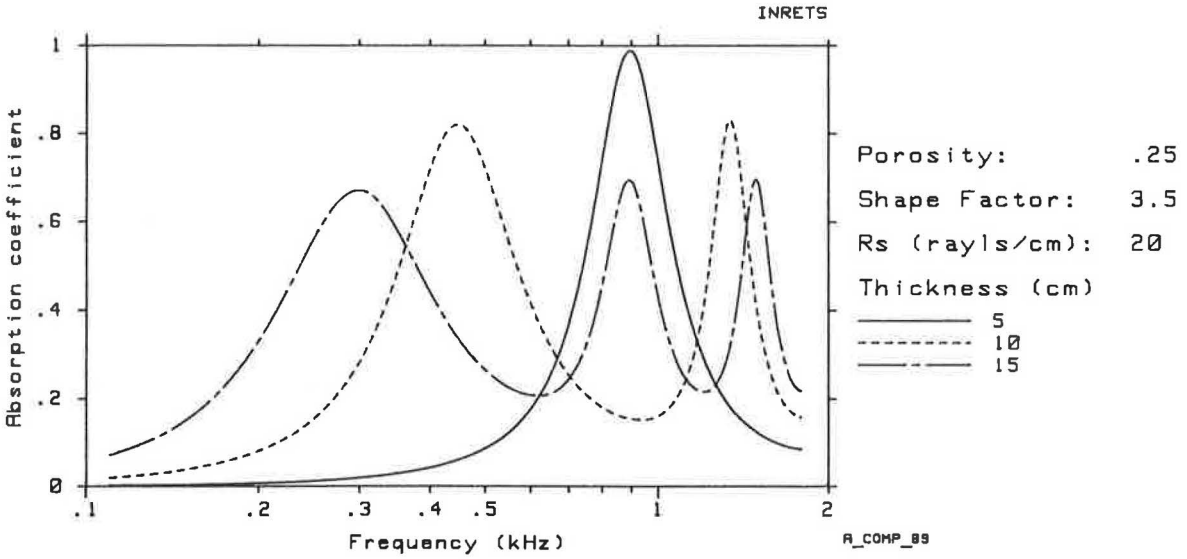

FIGURE 7 Influence of thickness on absorption.

which, using the high-frequency approximations (Equation 11) can be written

$$a_0 = 1 - \frac{\left(\frac{\sqrt{K}}{\Omega} - 1\right)^2 + \frac{1}{4K}\left(\frac{R_S}{\omega\rho}\right)^2}{\left(\frac{\sqrt{K}}{\Omega} + 1\right)^2 + \frac{1}{4K}\left(\frac{R_S}{\omega\rho}\right)^2}$$

The absorption increases monotonically with frequency (no oscillations) up to an asymptotic value $a_{0\,\text{asympt}}$, which happens to correspond to Equation 14. $a_{0\,\text{asympt}}$ does not depend on R_S. But, in terms of frequency, it will be reached "earlier" (i.e. at lower frequencies) if R_S is lower. (See Figure 8.) The curve corresponding to Equation 14 is given below (Figure 9). For a high absorption, one needs high Ω and low K. (Remember that $O < \Omega < 1$, $K > 1$.)

When is the superthickness condition reached? The condition $\coth(\gamma e) = \coth[(\alpha + i\beta)\, e] \rightarrow 1$ implies αe large enough. If not, the absorption curve will oscillate around the limit curve of Equation 17. The larger the αe, the smaller the amplitude of the oscillations. If the superthickness condition is practically said to be reached when the oscillation amplitudes become lower than 0.05 (the absorption coefficient does not differ by more than 0.05 from the limit values of Equation 17), this implies (7) that

$$\frac{R_S e}{\rho c}\frac{\Omega}{\sqrt{K}} \geq 3 \quad \text{super-thickness condition} \tag{18}$$

The thickness to be reached depends on the medium: if R_S is high, it can be a few centimeters. (See Figure 14.)

For a porous medium where $\Omega = 0.25$, $K = 3.5$, and $R_S = 20$ rayls/cm, one needs $e \geq 47$ cm (Figure 10).

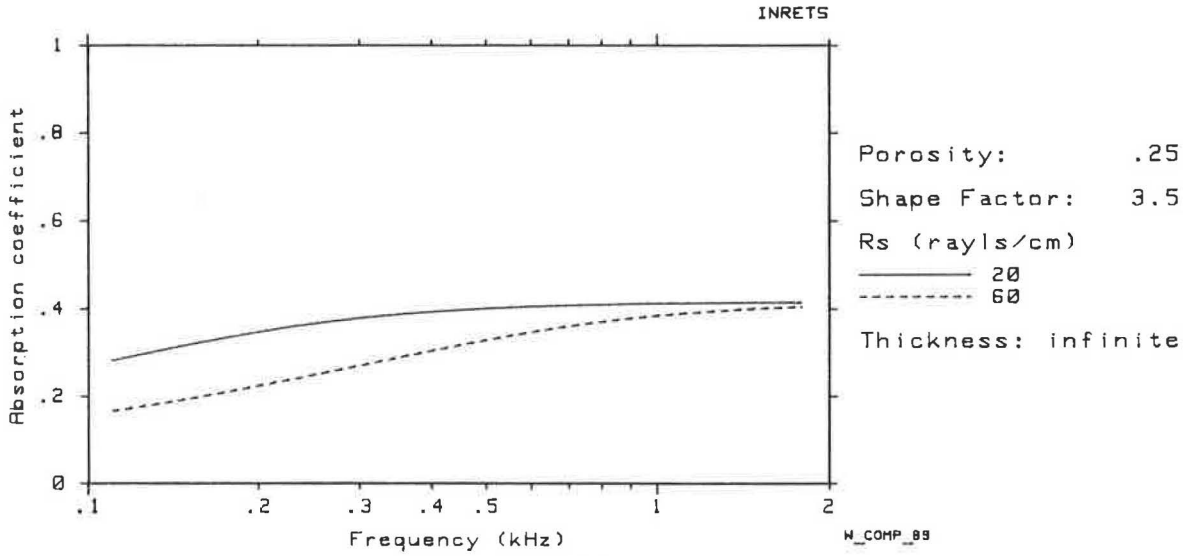

FIGURE 8 Influence of R_S on absorption for an infinite thickness.

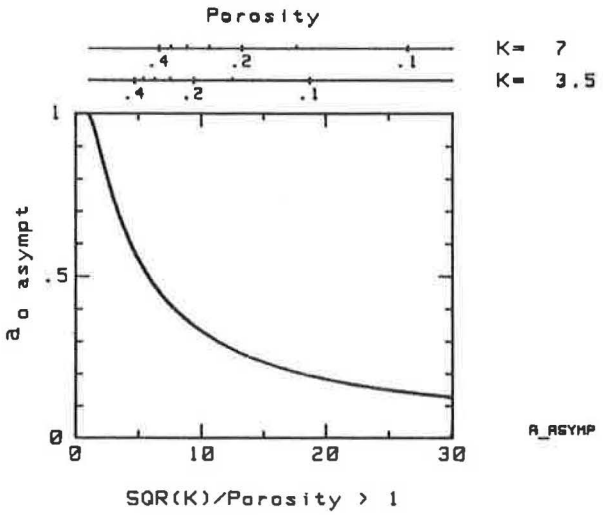

FIGURE 9 Asymptotic value of absorption (Equation 14).

Practically, for thickness

$$e \geq 3 \frac{\rho c}{R_S} \frac{\sqrt{K}}{\Omega} \tag{19}$$

- The absorption curve presents small oscillations, and
- Increasing the thickness will bring no practical improvement in the absorption.

EXPERIMENTAL VERIFICATION OF THEORETICAL MODEL

Experiments have been performed in the laboratory on single and multilayer samples (10-cm diameter) and outdoors on circular road tracks. Measurements on samples were essential to qualify the influence of the different physical parameters and study the effect of factors such as the number of layers, the humidity, the grading, and the binder. In situ measurements were taken afterwards, in order to verify the agreement between the laboratory results and those obtained on actual porous pavements.

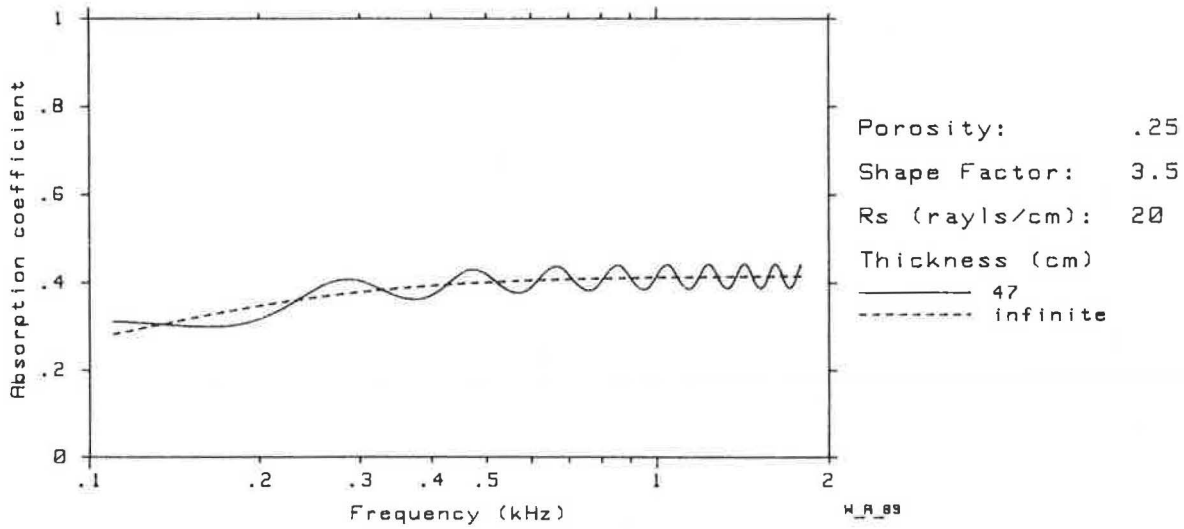

FIGURE 10 "Superthick" layer (47 cm) compared with an infinitely thick layer; absorption coefficient.

Influence of Physical and Intrinsic Parameters of Porous Asphalt Samples on Variation of Absorption Coefficient

The absorption coefficient measurement was carried out on laboratory samples by using the Kundt tube technique. The absorption coefficient is obtained from the maximum and the minimum sound pressure level values of the standing waves in the duct. In order to ensure as accurate measurements as possible, special care must be taken in positioning the sample at the duct end. Maximum and minimum sound pressure values must be precisely read.

As indicated earlier, the amplitude of the absorption peaks depends on the total airflow resistance $R_T = R_S \cdot e$ and is near unity for $R_T \approx 2\rho c = 83$ rayls cgs. In Figure 11, measurements are plotted with respect to frequency for two samples with $R_T = 93$ and 300 rayls cgs, respectively.

Reasonable agreement is found with theoretical curves. A small discrepancy at the higher frequencies may probably be attributed to the difference in the arrangement of the aggregates between the modeled structure and the experimental sample.

Observation of porosity influence could not be made; samples with $\Omega = 0.25$ and $\Omega = 0.35$, for instance, did not present the same shape factor ($K = 3.9$ and $K = 5.7$, respectively). The effect from the increase of Ω was partly "destroyed" by the corresponding increase of K.

The shape factor K directly influences the frequency positions of the absorption peaks. It depends on the sample composition (aggregate size and binder). In the experiments, the range of values was from 2.5 to 9. Figure 12 illustrates this phenomenon.

As shown in Figure 13, thickness has two effects:

- Modification of the frequencies of the absorption peaks: when e is doubled, the frequencies are shifted down by one octave (Equation 15), and
- Modification of the amplitude of the peaks: in the domain $R_T > 2\rho c = 83$ rayls, increasing the thickness diminishes the peak amplitude (minimum values of absorption are simultaneously increased).

When the thickness becomes large enough (superthickness condition, Equation 19), the result is a smooth curve increasing with frequency up to an asymptotic value (Equation 14). Such a phenomenon is observed in Figure 14 for a 15-cm-thick 0/2 porous sand asphalt sample (27 percent porosity) for which

$$\frac{R_S e}{\rho c}\frac{\Omega}{\sqrt{K}} = 30 >> 3$$

The superthickness condition is satisfied. (N.B.: The porosity comes from the absence of filler.)

The asymptotic value $a_{0\ \text{asympt}} = 0.54$ (from Equation 14) is not reached at 2,000 Hz because of the high value of R_S. (See Figure 8.)

For the tested formulations, double layers did not show crucial differences when compared with single layers (same overall thickness in both cases). Figure 15 shows the comparison of a single layer (0/10) and a double layer (0/10, 0/40) with an overall thickness of 16.5 cm in both cases. The expected difference (from theory) is higher than what is measured.

For layers with smaller grading difference [for instance, (0/10, 0.14) or (0/10, 0.20)], no experimental difference between single and double layers is observed. (See Figure 16.)

The humidity, grading, and binder content influence the a_0-curve mainly through the variation of the shape factor and partially through the variation of R_S and Ω, which are directly connected to the intrinsic characteristics of the internal structure.

In the presence of humidity, each parameter is affected differently. The global result is a drop in absorption and a

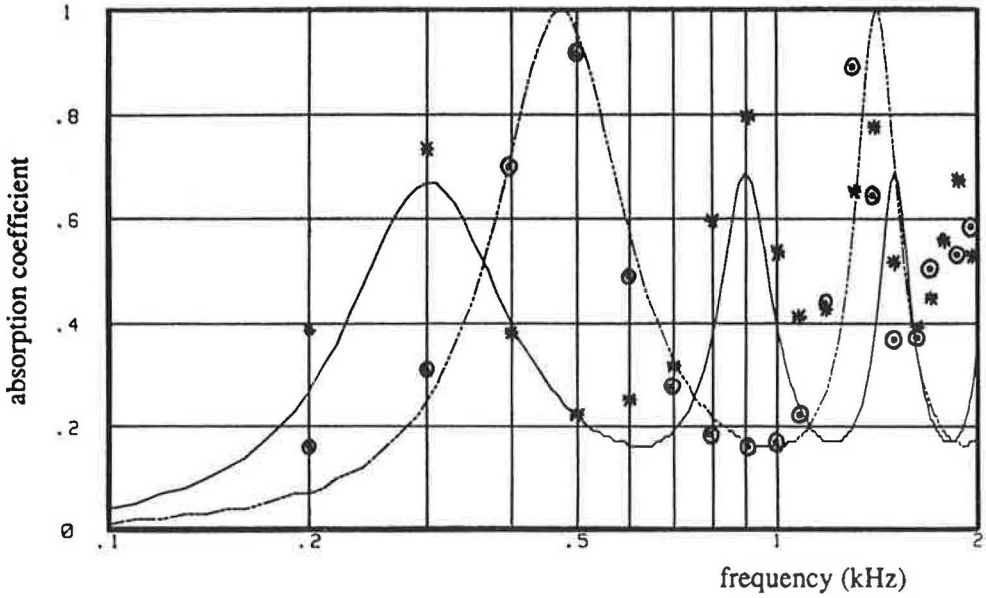

FIGURE 11 Influence of airflow resistance $R_T = R_S \cdot e$. ⊙ -----, $R_S = 8$ rayls/cm, $e = 11.6$ cm, $R_T = 93$ rayls. * ___, $R_S = 20$ rayls/cm, $e = 16.5$ cm, $R_T = 330$ rayls. $\Omega = 0.25$, $K = 3$. (When not specified otherwise, ⊙ and * are actual measurements and the dashed and solid lines are theoretical values.)

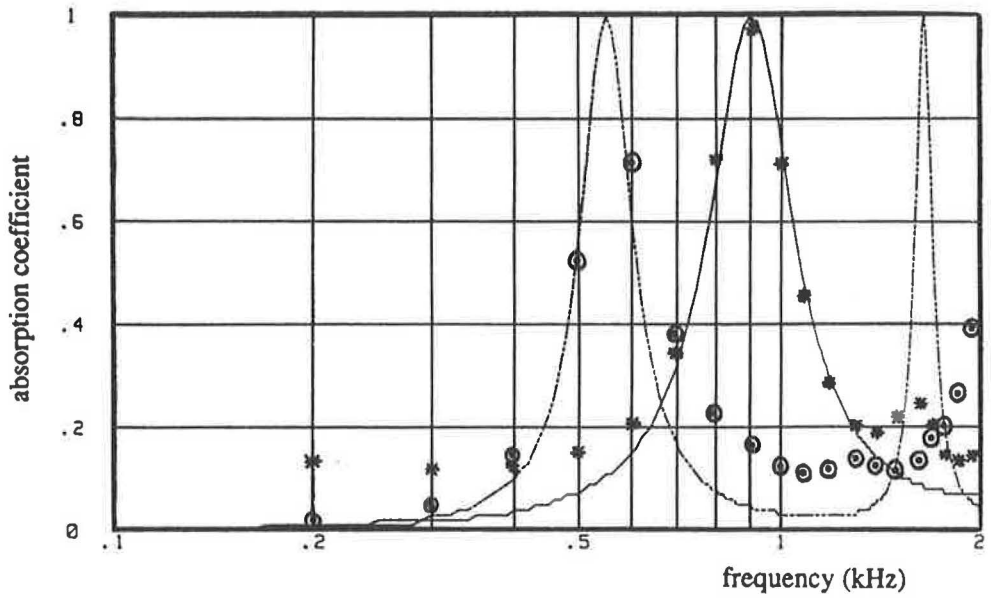

FIGURE 12 Influence of the shape factor K. * ___, K = 3.5; ⊙ -----, K = 9. R_S = 20 rayls/cm, e = 5 cm, Ω = 0.25.

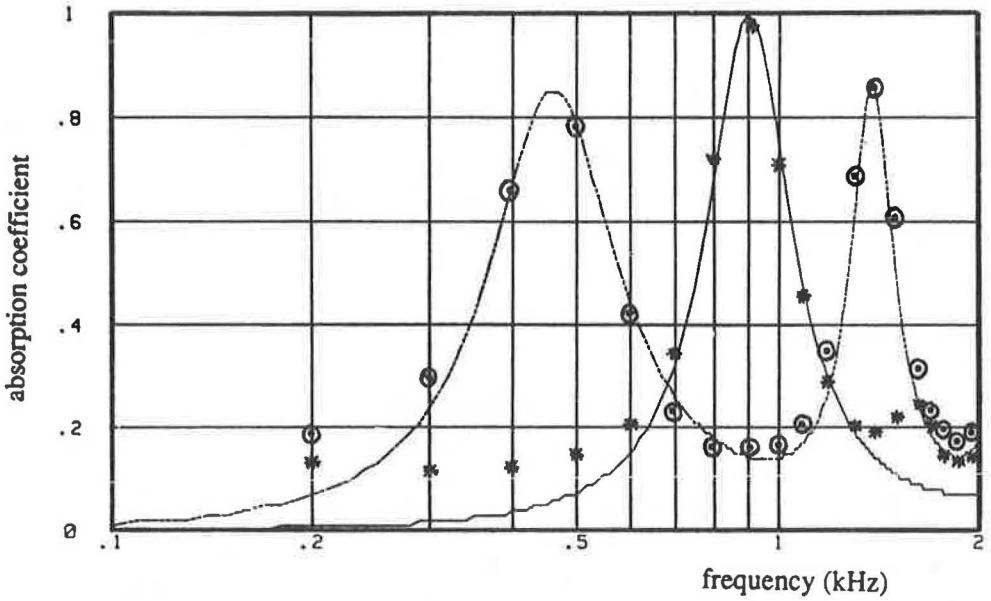

FIGURE 13 Influence of thickness. * ___, e = 5 cm; ⊙ -----, e = 10 cm. R_S = 10 rayls/cm, Ω = 0.25, K = 3.5.

shift of the peaks as shown in Figure 17. This fact must be taken into account, if it is considered that the pavements are not always completely dry.

For the experiments (Figure 17), measurements were first performed on a dry sample. The wet condition was achieved by immersing the sample in water, shaking it manually, and letting it dry naturally for one day.

As expected, the discontinuities in the grading do not seem to affect the absorption much. For a fixed grading (0/14), three different discontinuities were tested (2/4, 2/6, 2/10). The shape factor values were practically not affected (the measured relative variation was lower than 5 percent).

The modification in the binder content probably affects the direction and the section of the connections between the pores, which automatically changes the shape-factor value. This effect was already shown in Figure 12.

Outdoor Measurements

In order to qualify new porous asphalt roads, an important set of measurements was made. The aim of such a work was to test the reliability of the theoretical model for a large portion of the road (about 3 m²) and the representativeness of the small-sample measurement results (from a standing wave tube) to evaluate the global absorption coefficient of a road surface.

The measuring procedure used outdoors is based on an impulse technique (*16*): a_0 is evaluated from the transfer func-

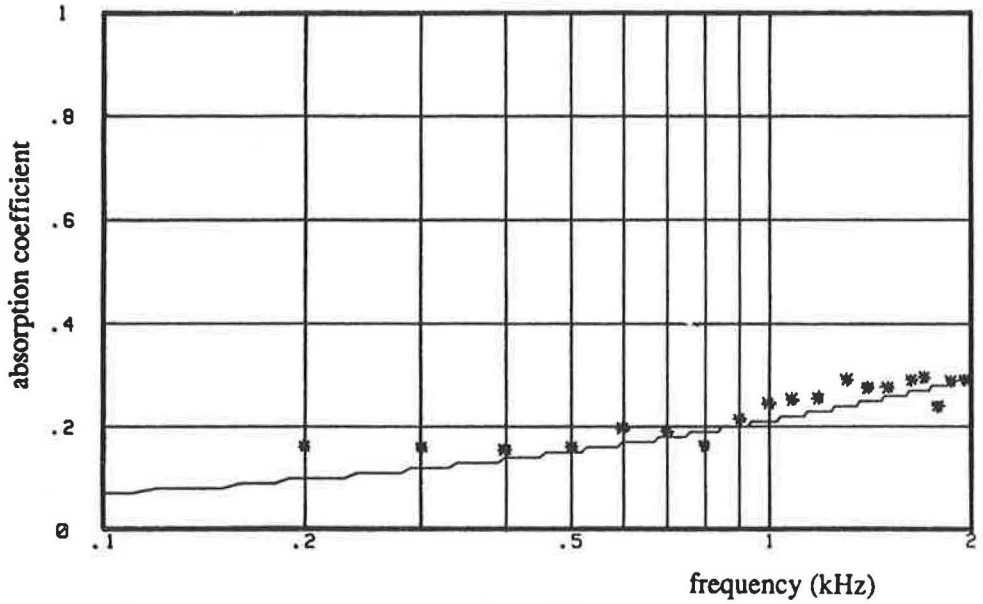

FIGURE 14 Superthickness effect. e = 15 cm, R_S = 440 rayls/cm, Ω = 0.27, K = 2.

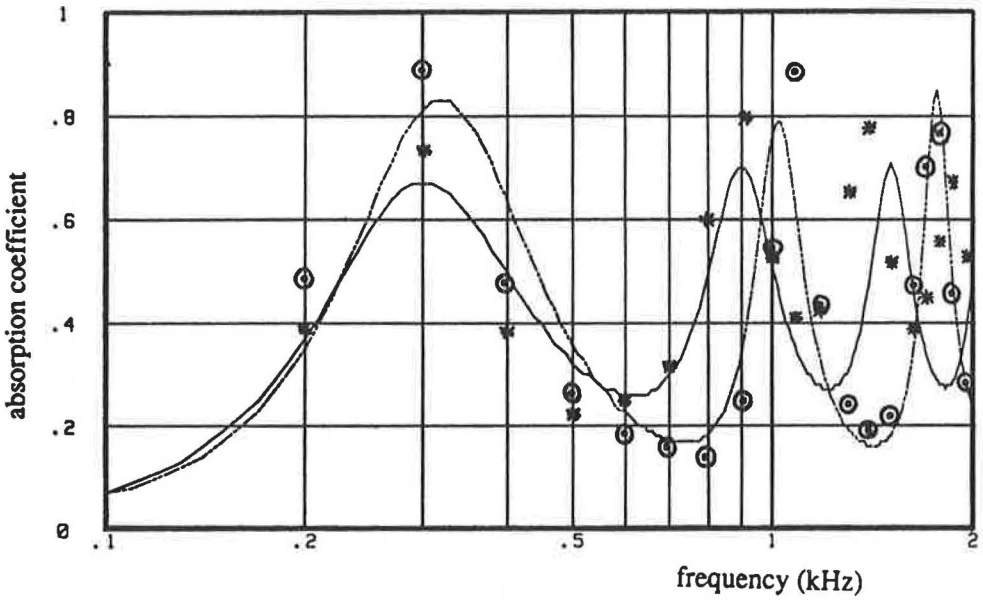

FIGURE 15 Double layer compared with single layer. * ___, single layer [1/10]; ⊙ -----, double layer [0/10, 0/40]. Same overall thickness: 16.5 cm.

tion, in normal incidence, between a direct and a reflected transient signal generated by an 8-mm alarm pistol. The results obtained by this technique compare well with those obtained with the standing wave duct on cores from the road (Figure 18).

However, one problem connected with the thickness of the wearing course must be pointed out. In road construction, the unevenness of the road base is taken care of by the porous asphalt (wearing course) spreading operation: the upper surface is made even. In the case of think layers, this means that for a 4-cm-thick layer, for instance, one can obtain 2.5 cm in one area and 4.5 cm at another. This discrepancy is not very important if acoustic measurements are made on a 3-m² area, but it can cause large differences on 10-cm-diameter samples (a large $\Delta e/e$ yields large differences in the absorption peak positions; see Equation 15). Such phenomena were noticed during the experiments on some of the 18 different porous surfacings on the French A63 Motorway (Bordeaux-Bayonne) and on some of the 12 tracks of the RN 76 (Bourges-Vierzon).

For thicker porous structures (>20 cm), this problem is avoided: on the one hand, owing to the low relative thickness difference (< 10 percent) and, on the other, because of the modification of the absorption curve. Such structures can be used to temporarily store rainwater. An example exists in the Loire Atlantique department in France, in the city of Rezé, where a complete porous structure 61 cm thick (35 cm of 10/80 crushed stone, 20 cm of 0/20 aggregate mixture with hard bitumen, and 6 cm of 0/14 porous asphalt). Figure 19

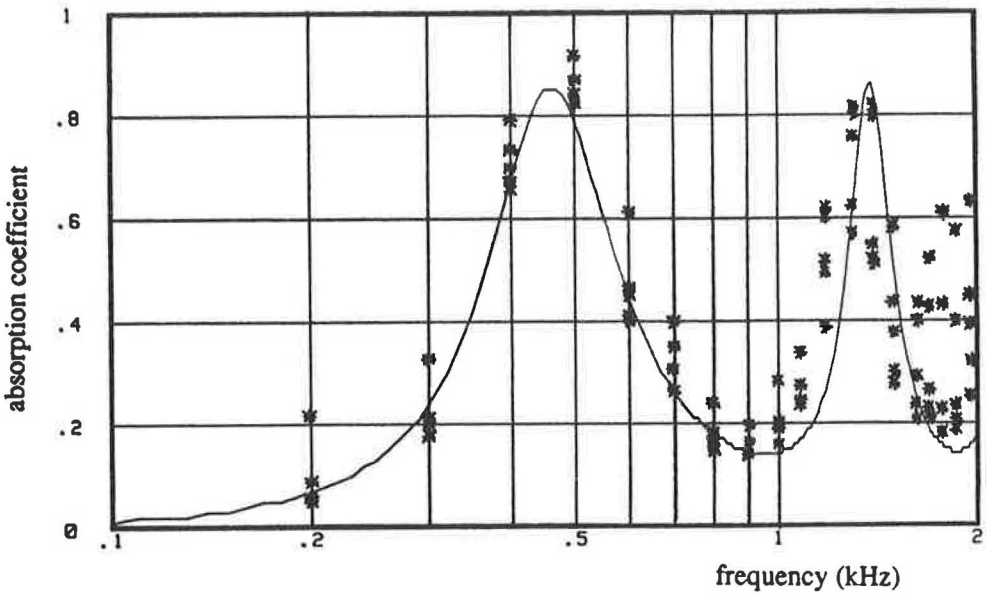

FIGURE 16 Double layer compared with single layer; *, double layer [0/10, 0/14] and [0/10, 0/20] measurements, ___, single layer [0/14], $R_S = 20$ rayls/cm, $\Omega = 0.25$, $K = 3.5$. Same overall thickness: 10 cm.

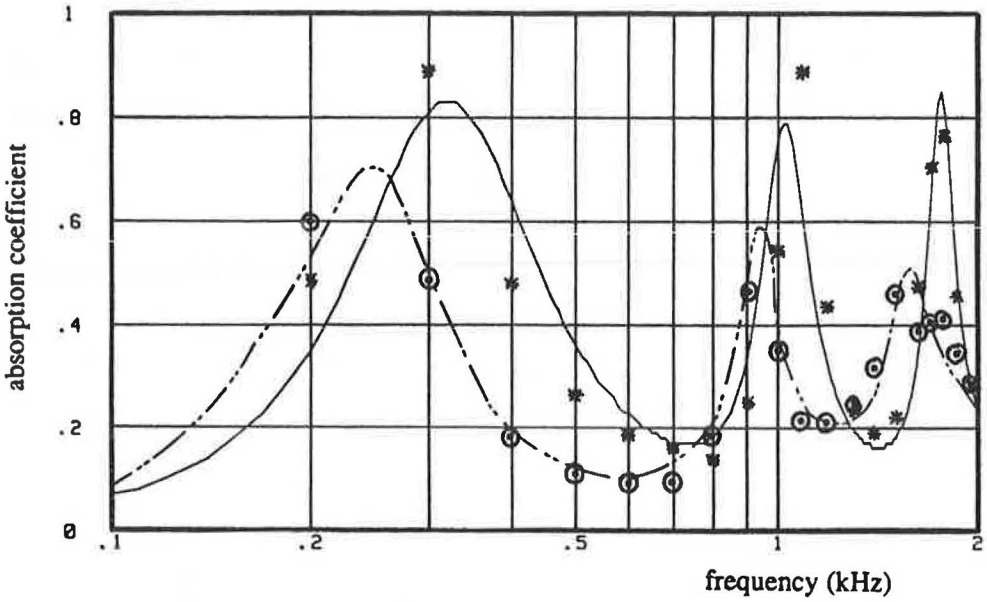

FIGURE 17 Humidity effect; -----, wet; ——, dry.

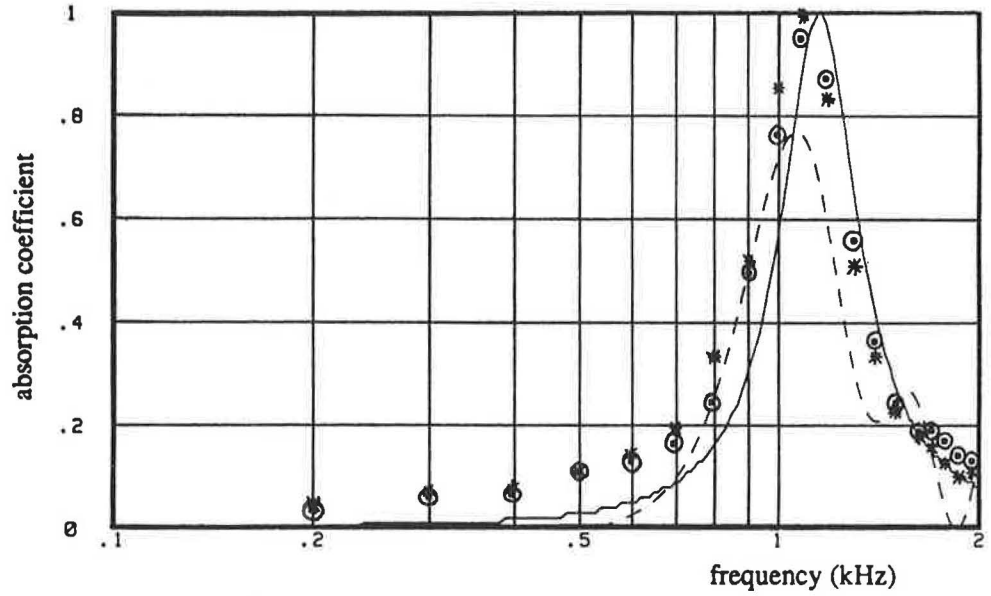

FIGURE 18 Absorption of some RN 76 wearing course. x, ⊙: standing wave results; -----: impulse technique; ——: theory.

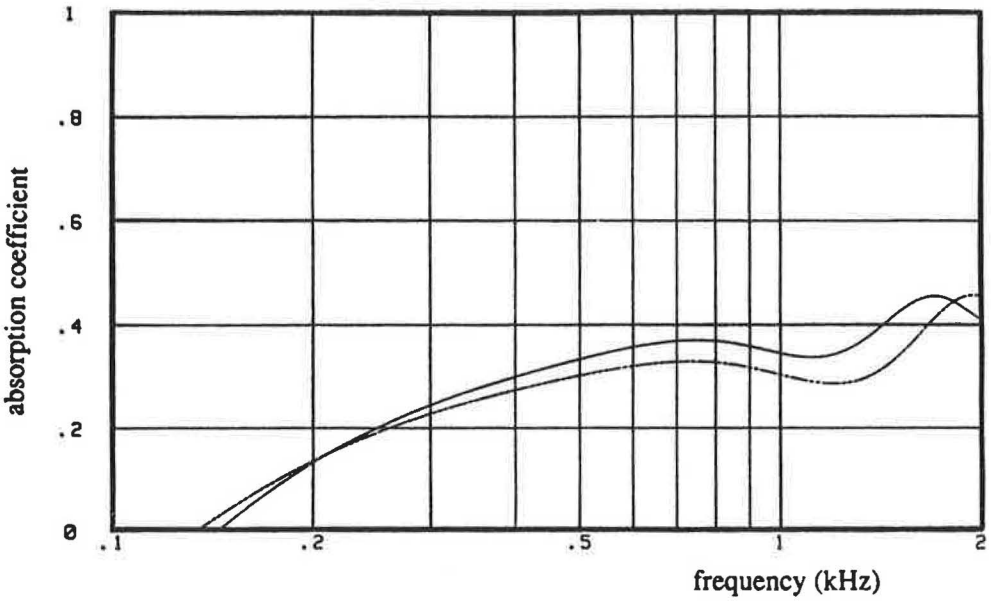

FIGURE 19 Absorption of a 61-cm-thick structure; measurements performed at two different locations in situ (Rezé, France).

presents the absorption coefficient measured at two locations using the impulse technique. This result is in good agreement with predicted and laboratory values.

Another experimental thick porous structure is in progress near Lyon. Theoretical investigations have been performed on the constitution of these porous structures in order to improve the acoustical properties.

The studies presented here deal with identification of the absorptive properties of porous asphalts and improvement of the composition. Knowledge of these characteristics is important for engineers, but it is obvious that qualification of the environmental impact on the neighborhood is also essential. This is the purpose of the next section.

ENVIRONMENTAL IMPACT OF A POROUS ASPHALT

Porous asphalts are becoming known as noise-reducing pavements. In fact, this quality results not only from their absorptive capacity, but also from the modification of the rolling noise source.

Basically (*17*), the acoustic emission is generated by a (tire) vibrating field and an air resonance process. The first is predominant in the low and medium frequencies (100 to 1200 Hz), and the other produces the main part of the energy in the high part of the spectrum.

On a concrete pavement or on a regular dense bituminous asphalt, the vibrations come from tire strains during rolling, the impact of the tire treads on the road, and the slip-and-stick effect. The air resonance is mainly generated by air pumping. Because of their porosity, porous asphalts behave differently. On the one hand, the vibrations transmitted to the tire are less important owing to a lower surface texture (and consequently a lower indenting of the aggregates in the tire surface), which can induce adhesion problems at low speeds, and a reduction of the slip-stick phenomenon. On the other hand, air pumping is widely reduced.

All these factors affect tire noise generation and are the main reason for the noise reduction. The other reason is the absorption of the structure itself. The excess attenuation is caused by the absence of multireflections between the tire and the road (horn effect) (*18*) and between the body of the vehicle and the road. If one takes into account both phenomena (low rolling noise and absorption effect), one measures, following ISO R 362 (coast-by method), for a single vehicle, a noise level that is approximately 2 or 3 dB(A) below the noise level found for a dense bituminous asphalt. This is a mean value obtained from about 20 measurements on thin-layer surfaces. When the porous structure is thick (around the superthickness condition), the absorption is almost constant on the whole frequency range ($\alpha \sim 0.4$ to 0.5) (Figure 19), which yields better excess attenuation. In this particular case, the global attenuation reaches 5 to 6 dB(A) (*19*).

To take into account a more realistic traffic flow, two vehicles (with engine on) and three types of tires are used. The noise level at 90 km/hr is estimated by linear regression on the maximum sound pressure level values ($L_{p\ max}$) for several (constant) speeds between 70 and 110 km/hr. This method was first tested in a French-German twin cooperation framework (tests done in 1986 near Strasbourg, France, with 15 vehicle-tire configurations on five different experimental tracks (*20*)). Round robin tests are performed on real roads.

Porous Asphalt in an Urban Area

One application of such noise-reducing pavement is in urban areas, particularly on the streets with buildings on each side. In this case, there is an important number of reflected paths. According to the acoustic condition in a diffuse field (*21*), one can expect that an absorbing pavement can "trap" partially or completely, depending on the thickness of the structure, the acoustic energy after a few reflections.

Some calculations of the acoustic field in a canyon street with an absorbing pavement, using a finite-element technique with a complex acoustic source (one spherical source for the radiation of each tire and one for the engine) show that the acoustic level in front of the facades relative to the level in the same street with a nonabsorbing pavement (dense bituminous asphalt, for example) is inferior by several decibels: 1 to 6, depending on the thickness of the absorbing layer.

The physical theory is similar to the one used in room acoustics. In this case, the lower surface is covered with an absorbing material (porous asphalt), and the top surface has an impedance = ρc. The facade surfaces are perfectly reflective.

One experiment has already been conducted in Paris (*22*); two others are in progress in Paris and Nantes on different types of road systems with different traffic volumes. For each case, an adequate thickness is investigated. Acoustic measurements must be performed day and night before and after construction in order to evaluate the gain on a real traffic flow. In parallel with those measurements, inquiries are being made among the neighbor population as to the subjective impact. Inquiries are focused not only on the acoustical aspect, but also on other factors such as water spray, aquaplaning, comfort, and so forth.

The first results will be published in 1990.

Evolution of Noise Level Versus Pavement Aging

In the first 6 months after spreading, the porous asphalt evolves quickly, producing a modification in the mechanical properties of the structure and also in the rolling noise level. With the single car coast-by method (80 km/hr, tires under 5,000 km wear), the difference between two sets of measurements (the second set is made 6 months later) can approximately reach ± 2 dB; these observations were made on the 18 surfacings of the French A 63 motorway (Bordeaux-Bayonne) (See Figure 20). After 1 year under traffic, the evolution of the acoustic level is less important (within 1 dB). Nevertheless, it is necessary to pay attention to the clogging, which can transform an open pavement into a dense one and in the same way increase the noise level. Our experience on motorways shows that the clogging is not very important in the rolling tracks when the road is continuously trafficked. In this case, there is a self-cleaning of the pores by the tires themselves. In urban areas, not enough information is available, but it seems that clogging is a more worrisome problem than on suburban or country roads.

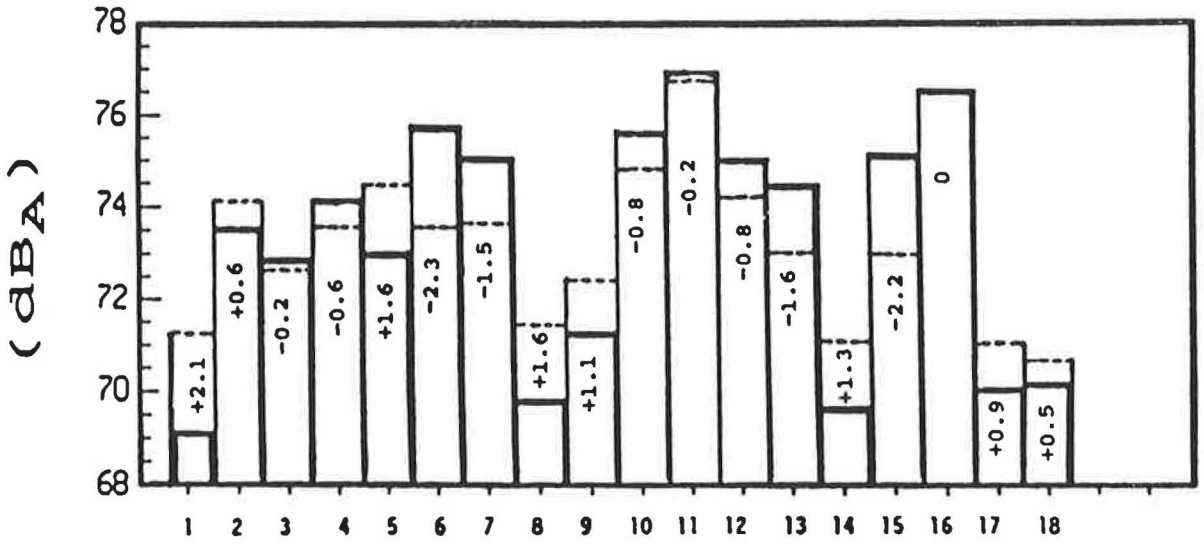

FIGURE 20 Evolution of the acoustic behavior of porous asphalt in the first year measured on 18 surfacings: ——, first set; -----, second set (6 months later).

In any case, it is necessary to follow the acoustic evolution of all the sites on which work was done. More elements should be available in the next 3 or 5 years.

Case of Heavy Vehicles

The results presented in this paper concern light vehicles, the main acoustic source (more than 60 km/hr) for which is rolling noise. This source is very near the surface and, therefore, the noise propagation is largely affected by the presence of the absorbing pavement.

For diesel heavy vehicles, the noise source is differently located. The rolling noise is in fact responsible for a small part of the global acoustic energy (*3*), which is mainly produced by the engine and the mechanical noise (vibrations, gears, brakes, maybe exhaust); that is why it is believed that the influence of an absorbent pavement on heavy vehicle noise is less important. Nevertheless, the absorbing effect on the multi-reflections between the body of the vehicle and the road is still effective. But for how much?

More studies on this topic are in progress; it is hoped that the first results will be available very soon.

CONCLUSION

The calculations and measurements presented in this paper permit the conclusion that a porous asphalt can be realistically modeled by physical parameters: airflow resistivity (R_S), porosity (Ω), shape factor (K), and thickness (e), and, that its environmental impact can be very important. Following the type of road, the vehicle speed, type of vehicle, noise mechanisms, and source location, the porous asphalt pavement can be more or less efficient. At any rate, it seems that the gain is always positive. The excess attenuation is between 1 and 6 dBA.

All the acoustic properties combined with good adhesion in the high-speed domain, good visibility on rainy days, and the elimination of water spray and aquaplaning according to the drainage qualities suggest that porous asphalt will be widely used in the future.

REFERENCES

1. *XVIIIth World Road Congress, Surface Characteristics*. Permanent International Association of Road Congresses, Brussels, Belgium, Sept. 1987, pp. 61–75.
2. G. Gachignard and P. Sardin. Influence de la nature de la chaussée sur le bruit produit par le contact pneumatique-chaussée. *Bulletin de Liaison, Laboratoire Central des Ponts and Chaussées* (LCPC), Paris, 1974.
3. Y. Delanne. Bruit routier et revêtements des chaussées. *Revues Générales des Routes et Aérodromes*, No. 637, Jan. 1987, pp. 45–51.
4. P. Bar. *Pour une Perspective de Recherche sur l'Utilisation des Chaussées Poreuses en Vue de Réduire le Bruit en Ville*. Rapport CETUR. Centre d'Etudes des Transports Urbains (CETUR), Bagneux, France, 1988.
5. *Note d'Information SETRA: Enrobés Drainants*. No. 40, Série Chaussées-Dépendances. Société d'Etudes et de Travaux, March 1988.
6. J. F. Hamet. *Modélisation Acoustique d'un Enrobé Drainant—Etude Théorique en Incidence Normale*. Rapport INRETS 59. Institut National de Recherche sur les Transports et leur Sécurité (INRETS), Bron Cédex, France, 1988.
7. J. F. Hamet. Modélisation Acoustique d'un Enrobé Drainant—La Super Épaisseur. NNB 8901. INRETS, Bron Cédex, France, 1989.
8. M. Berengier, Y. Delanne, P. Daburon, and P. L'Hermite. Chaussées peu Bruyantes. Contribution du LCPC, Rapport LCPC. LCPC, Paris, 1989.
9. M. E. Delany and E. N. Bazley. Acoustical Properties of Fibrous Materials. *Applied Acoustics*, Vol. 3, 1970. p. 105.
10. K. Attenborough. Acoustical Characteristics of Porous Materials, *Physics Reports*, Vol 82, 1982, p. 3.
11. P. M. Morse and K. U. Ingard. *Theoretical Acoustics*. McGraw-Hill, New York City, 1968.
12. A. Von Meier. A Poro-Elastic Road Surface for Traffic Noise Reduction. *Internoise*, 1985, pp. 287–290.
13. *Banc Gamma Vertical A 322 b*. LCPC, Paris, France.

14. *Acoustics—Materials for Acoustical Applications: Determination of Airflow Resistance*. ISO/DIS 9053. International Standards Organization, 1988.
15. T. Bourbie, O. Coussy, and B. Zinszner. *Acoustique des Milieux Poreux*. Editions Technip., 1986.
16. M. Berengier and Y. Delanne. Caractéristiques acoustiques intrinsèques d'une structure par une méthode impulsionnelle. *Bulletin de Liaison, LCPC*, Vol. 139, Sept.–Oct. 1985, pp. 113–118.
17. Y. Delanne. Les enrobés drainants: Analyse de leur propriétés vis-à-vis du bruit de roulement et de l'adherence des pneumatiques des véhicules de tourisme. *Bulletin de Liaison, LCPC*, Vol 162, 1989, pp. 33–43.
18. K. Schaaf and D. Ronneberger. Noise Radiation from Rolling Tires: Sound Amplification by the "Horn Effect." *Internoise*, 1982, pp. 131–134.
19. M. Berengier, J. F. Hamet, P. L'Hermite, and P. Daburon. L'acoustique des revêtements routiers poreux. *Proceedings, 13th International Congress on Acoustics*, Belgrade, Vol. 2, 1989, pp. 51–54.
20. *Expérimentation France-Allemande de la Wantzenau*. Rapport de Synthèse Français. CETUR, Bagneux, France, 1988.
21. R. H. Lyon. Role of Multiple Reflections and Reverberation in Urban Noise Propagation. *Journal of the Acoustical Society of America*, Vol. 55, 1974, pp. 493–503.
22. Y. Delanne and R. Lebret. Efficacité acoustique des enrobés drainants. *Revues Générales des Routes and Aérodromes*, No. 653, 1988.